Investigation of A City-scale Three-dimensional Macroscopic Fundamental Diagram for Bi-modal Urban Traffic

Nan Zheng, Konstantinos Aboudolas, and Nikolas Geroliminis

Abstract - **Recent research has demonstrated that the Macroscopic Fundamental Diagram (MFD) is reliable and practical tool for modeling traffic dynamics and network performance in single-mode (cars only) urban road networks. In this paper, we first extend the modeling of the single-mode MFD to a bi-modal (bus and cars) one. Based on simulated data, we develop a three-dimensional MFD (3D-MFD) relating the accumulation of cars and buses, and the total circulating flow in the network. We propose an exponential function to capture the shape of the 3D-MFD, which shows a good fit to the data. We also propose an elegant estimation for passenger car equivalent of buses (PCU), which has a physical meaning and depends on the bi-modal traffic in the network. Moreover, we analyze a 3D-MFD for passenger network flows and derive its analytical function. Finally, we investigate an MFD for networks with dedicated bus lanes and the relationship between the shape of the MFD and the operational characteristics of buses. The output of this paper is an extended 3D-MFD model that can be used to (i) monitor traffic performance and, (ii) develop various traffic management strategies in bi-modal urban road networks, such as redistribution of urban space among different modes, perimeter control, and bus priority strategies.**

I. Introduction

To understand the physics of urban mobility, traffic dynamics of urban networks with multiple modes need to be analyzed under various network structures. As multiple modes compete for limited urban space, conflicts and interactions are developed resulting in congestion. Existing literature on multimodal traffic mainly focuses on design and operation of special lanes [1], [2], optimization of signal control [3], [4], etc. However there is no significant body of work dedicated on the modeling of traffic dynamics and the influence of each mode on the network performance. Most of the existing works fall short either in the scale of application or the treatment of congestion dynamics (small scale and/or static models). For example, reference [2] estimates traffic state for each mode based on a type of model which works only for uncongested and static conditions. References [1], [5] are based on the link-scale Fundamental Diagram, which can experience high scatter and therefore cannot provide accurate estimates of speed and travel time. These microscopic models are also computationally complex when applied at network scale. Macroscopic approach can overcome these problems with less cost. The idea of macroscopic traffic model for car-only urban networks has been initially proposed in [6] and was re-initiated later in [7], [8]. The demonstration of the existence with dynamic features and filed data of the Macroscopic Fundamental Diagram (MFD) is recent [9]. This work showed that: (i) urban single-mode regions exhibit an MFD relating network space-mean flow and density, (ii) the MFD is a property of the network itself. Recent work also highlighted that the spatial distribution of congestion can affect the shape and the scatter of the MFD [10], [11]. Analytical theories have been derived for the shape of the MFD as a function of network and intersection parameters, using variational theory for homogeneous and heterogeneous network topologies [12], [13]. The properties of a well-defined MFD, stability and scatter phenomenon are analyzed through many other simulation studies and experimental tests [14], [15], [16], [17], [18], [19]. Given the MFD of a network, effective traffic management strategies can be readily developed to mitigate congestion, examples including perimeter flow control [20], [21] and cordon-based pricing [22].

Building on the knowledge of the single-mode MFD, developing and understanding the dynamics of multimodal networks is promising. In this paper, we seek to extend the modeling and the application of the single-mode MFD to a bi-modal (bus and cars) one, with the consideration of passenger flows and traffic performance of each mode. The dynamics of traffic flow in a bi-modal network are more complicated due to the operational characteristics of buses and the interactions between cars and buses. Despite of this complication, simulation studies on small networks show that a classical MFD applies (under certain conditions) for bi-modal urban networks [23], [24] as well. However, the influence of each mode in the network dynamics and performance is still missing. This relationship, if known, will facilitate the development of control strategies at various levels, e.g. network bus priority or redistribution of urban space [23], [25]. Therefore we aim at investigating the relationship among the accumulation of cars and buses, and the traffic throughput or circulating flow of a network. Because of different interactions for different congestion levels, it is insufficient to assume a state independent value for the Passenger Car Unit (PCU) equivalent. Furthermore, buses are usually considered to travel at constant speed without dynamics when operating on dedicated bus lanes (see e.g. [4]). This is insufficient, as the buses flow dynamics are influenced not only by periodic stop-and-go phenomena at signalized intersections, but also the operational delays incurred at bus stops and interaction of the multimodal traffic (e.g. buses left turns). These dynamics are rarely studied and have to be further investigated.

The rest of the paper is organized as follows: Section II investigates the existence and the properties of a bi-modal MFD by simulation studies. Section III extends the bi-modal

N. Zheng, K. Aboudolas, and N. Geroliminis are with the Urban Transport Systems Laboratory, School of Architecture, Civil & Environmental Engineering, École Polytechnique Fédérale de Lausanne, CH-1015 Lausanne, Switzerland(E-mail: nan.zheng@epfl.ch, konstantinos.ampountolas@epfl.ch, nikolas.geroliminis@epfl.ch)

MFD modeling from vehicle to passenger flows. Section IV looks at the dynamics of buses on dedicated bus lanes and the properties of a bus-only MFD. Section V summarizes the findings and discusses policy indications.

II. The Existence of City-Scale Bi-modal Macroscopic Fundamental Diagrams: Simulation Findings

In this section, we investigate the relation among accumulation of cars and buses and vehicle flow in bi-modal traffic networks via simulation experiments. We show that a large-scale test site exhibits a city-scale three-dimensional MFD (3D-MFD) relating the accumulation of cars and buses to flow with moderate scatter under different bi-modal demand patterns. Finally, we investigate different functions to approximate the shape of the 3D-MFD, so that to be integrated in a traffic management framework.

A. *Site and simulated Data*

The test site is a 2 km^2 area of Downtown San Francisco including about 100 intersections and 430 links of total 101 lane-km.The traffic flow in the (bi-modal) network comprises two vehicle classes, i.e., passenger cars and buses. Let us denote by n_c the accumulation of cars and n_b the accumulation of buses, and Q the total network flow (in vehicle per unit time) which is the sum of car and bus flows. For the developed model, the flow Q in the bi-modal network is considered to be a function of n_c and n_b given by

$$Q = Q(n_c, n_b). \quad (1)$$

To obtain the shape of (1) we perform extensive simulation experiments in the test network with time-dependent asymmetric origin-destination tables, starting from different initial compositions of the bi-modal traffic (pairs of n_c and n_b). The initial profile for cars is a typical peak-hour demand with a trapezoidal shape. For buses, the demand is determined by the number of lines and their operational frequency. For the simulation experiments, the test network is modeled via the AIMSUN microscopic simulator. The simulation horizon for each experiment is 5.5 h and pairs of data (n_c, n_b) are gathered every 5 min from the simulator. For each 5min interval, total flow Q' is estimated from the simulator.

Fig. 1(a) depicts the projection of the 3D diagram on the (n_c, n_b) plane. This projection shows the generated pairs of n_c and n_b for different demand patterns. It should be noted that more than 20 runs with different bus frequencies were carried out to generate different mode compositions and obtain the corresponding traffic performance Q'.

Fig. 1(b) illustrates the 3D-MFD for bi-modal traffic resulting pattern. As a first remark, Fig. 1(b) confirms the existence of a 3D-MFD like-shape for bi-modal networks, whose exact shape is seen to depend on the accumulation of cars and buses. To enable a better understanding of this figure, Fig. 1(c) displays the contour plot of the 3D-MFD on the (n_c, n_b) plane, using an interpolation algorithm to estimate flow in a continuous space of the accumulation plane. The triangle in this figure indicates the bi-modal traffic composition where the network operates close to the maximum throughput of the 3D-MFD. In particular, it captures the "optimal operational region" of bi-modal traffic. City managers and practitioners could seek to derive management strategies to operate at this optimal regime. It can be seen that the flow Q' decreases monotonically as n_c and n_b increases, albeit with different slopes. Remarkably, the slope of buses is higher that the slope of cars. This indicates that effect of an additional bus in the network is much different than an additional car. This property is investigated more in Section II.C. A simple explanation is that buses make additional to traffic signal stops for passengers, and negatively influence traffic and create stop-and-go phenomena. The figure also depicts critical accumulations of cars $\tilde{n}_c$ (rising line in the triangle) where Q' reaches its maximum for different values of n_b. The slope of the rising line reflects that the capacity to servecars has to be compromised in order to serve more buses. As a general remark, the 3D-MFD can be used by policy makers to exploit the trade-off between the operation of buses and cars and design more sustainable cities. Note also that the maximum value of the network flow occurs for $n_b = 0$ and $n_c = 3500$ because of the effect of bus stops. As we will show later, a consideration of different vehicle occupancies for buses and cars and the estimation of network passenger flow will produce a completely different result.

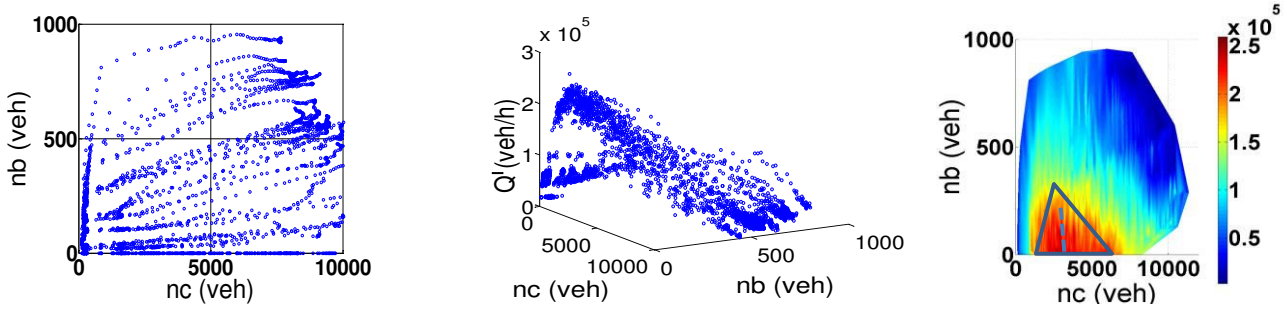

Fig. 1. (a) Generated pairs of $n_c$and n_b; (b) The 3D-MFD points for bi-modal traffic; (c) Contour plot of the 3D-MFD after interpolation

B. An Exponential Flow Model for Bi-modal Vehicle Traffic

Given that evaluating $Q(n_c, n_b)$ in (1) for many pairs of n_c and n_b is tedious, we propose instead using an exponentialflow model that approximates the 3D-MFD in Fig. 1(b). This task is challenging because the ultimate goal is the derivation of a generic 3D-MFD formula with two variables and a few parameters that can be used to improve accessibility in bi-modal traffic networks. To this end, we consider the following exponential flow function for data fitting:

$$Q(n_c, n_b) = a(n_c + n_b)e^{bn_c^2 + cn_b^2 + dn_c n_b + en_c + fn_b} \quad (2)$$

where a, b, c, d, e, f are model parameters. The parameter values should be specified so as to minimize the deviation of model (2) from the corresponding measured values Q'. This function can be considered as a generalization of the Drake's exponential function for a 2D single point fundamental diagram. An unconstrained estimation will not be consistent with the physics of traffic and constraints (3) are added. To this end, we estimate the values by Least-Squares parameter estimation for the given simulated data Q' in Fig. 1(b). The parameter estimation problem is formulated as follows (P1):

$$\min_{a,b,c,d,e,f} Z = \|\boldsymbol{Q} - \boldsymbol{Q}'\|^2$$

Subject to (3)

$$\begin{cases} Q \geq 0 & \dfrac{\partial V}{\partial n_c} \leq 0 \quad \dfrac{\partial V}{\partial n_b} \leq 0 \\ \dfrac{\partial PCU}{\partial n_c} \leq 0 & \dfrac{\partial PCU}{\partial n_b} \leq 0 \end{cases}$$

where V is the space-mean speed in the network, PCU is the Passenger Car Unit equivalent value, and $\boldsymbol{Q}, \boldsymbol{Q}'$ are vectors with elements of the model (2) and the simulated data Q' for each 5 min sample interval, respectively. Variable $V(n_c, n_b) = QL/(n_c + n_b)$ by definition, where L is the average link length of the network. The first constraint in (3) guarantees non-negative flows. The second and the third constraint say that the space-mean speed of all vehicles should decrease monotonically as n_c and n_b increase. Finally, the last two constraints ensure that the PCU is state-dependent and should monotonically decrease as n_c and n_b increase, as well. The estimation of the PCU will be discussed in the next section.

The parameter estimation problem (P1) is nonlinear and can be readily solved by public or commercial software. The estimated parameters resulting from the optimization problem read: a, b, c, d, e, f = 1.95e02, -2.34e-09, 5.28e-07, 6.34e-08, -2.92e-04, -1.50e-03. Fig. 2(a) illustrates the results of fitting model (2) with the estimated parameters to the simulated data. An R-square value of 0.91 (close to 1) indicates that the resulting 3D-MFD fits well with the data and all physical constraints are satisfied. Note that a slice of the 3D-MFD in Fig. 2(b) for a fixed value of n_b results to the unimodal MFD of urban traffic. Fig. 2(b) depicts the contour plot of the 3D surface on the (n_c, n_b) plane. Comparing Fig. 2(b) with Fig. 1(c), we can see that most patterns observed closely matches each other except the area for very high values of buses $n_b > 600$ due to lack of simulated data. Nevertheless, these states cannot be easily observed in real systems. Moreover, it can be seen that the "optimal operational region" (triangle in Fig. 1(c)) of bi-modal traffic is reproduced in a very similar way. Fig. 3(a) shows the 3D-MFD relating n_c and n_b with the space-mean speed V in the network. It can be seen that the space-mean speed decreases monotonically as n_c and n_b increases.

C. PCU Value Estimation in Bi-Modal Networks

Recent research has proposed simple models relating the different modes of traffic with their space-mean speeds in multimodal networks [23]. These models indicate that the PCU value for buses becomes smaller as congestion increases, because the effect of bus related stops is a smaller part of the total travel time. Thus, a static PCU consideration is insufficient to reflect the dynamic relationship between buses accumulation and congestion. For this reason, we analytically estimate the PCU value as a function of accumulation of cars and buses: PCU is estimated as follows: For any pair of (n_c, n_b) there is a pair $(n_{c0}, 0)$ that satisfies $V(n_{c0}, 0) = V(n_c, n_b)$, where n_{c0} is the uni-modal traffic, i.e., the accumulation of cars provided $n_b = 0$. Thus, $PCU(n_c, n_b)$ is the solution of the equation $n_{c0} = n_c + PCU \cdot n_b$. Then the average speed can be rewritten as:

$$V(n_c + PCU \cdot n_b, 0) = V(n_c, n_b) = \frac{QL}{n_c + n_b} \quad (4)$$

Combining (2) and (4), we obtain the solution of PCU. Fig. 3(b) displays PCU for different values of n_c and n_b. Note that the resulting PCU satisfies the last two constraints in (3).

III. Derivation of a City-scale Bi-modal Macroscopic Fundamental Diagram for Passenger Flows

Given the 3D-MFD (2) of a network with cars and buses, incoming flow can be controlled at the boundary of the network in order to direct the network operates at its "optimal

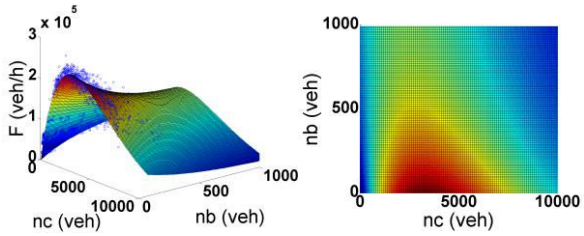

Fig. 2. (a) The approximated 3D-MFD; (b) Contour plot of the 3D-MFD on the (n_c, n_b) plane.

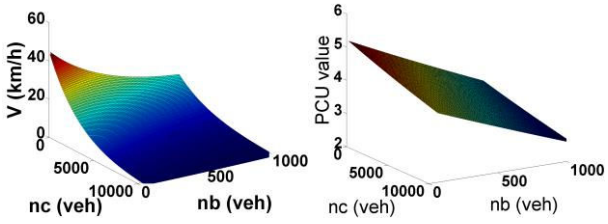

Fig. 3. (a) The 3D-MFD relating accumulation of cars and buses with space-mean speed; (b) A 3D diagram relating accumulation of cars and buses with PCU.

operation region". Existing methodologies for car-only perimeter control can be found in [20], [21], [26] and elsewhere. Based on this MFD, however, it is possible that a controller would always try to restrict bus flow from entering the network. This is due to the monotonic relation between bus accumulation n_b and the flow Q. From a passenger mobility perspective, this control strategy cannot optimize network conditions as it will not consider the buses are more efficient modes, due to higher passenger occupancy. To maximize the passenger flow of a network and thus realize the efficiency of a multimodal network, we shall need a bi-modal MFD that can capture the dynamics of passenger flows. In this section, we first describe a derivation of the analytical form of the passenger flow 3D-MFD based on the vehicle flow 3D-MFD. And we further show that our test site exhibits a city-scale 3D-MFD relating the accumulation of cars and buses to passenger flow, as well.

A. The Derivation of a Bi-Modal MFD for Passenger Flow

Denote P the passenger flow in the bi-modal network, with n_c and n_b, $P = P(n_c, n_b)$. Denote h the average number of on-board people per vehicle, the occupancy**.** We assume that car occupancy h_c is constant h_c =1.3, while we estimate bus occupancy h_b with a model proposed in [23], as a function of the dwell time. Denote speed of car v_c and bus v_b, the flow of cars Q_c and buses Q_b. By definition, total passenger flow P can be written by (5):

$$P = h_c Q_c + h_b Q_b \tag{5}$$

Given the analytical form of Q in (2), we try to estimate Q_c and Q_b for each mode by Q, n_c and n_b. To this end, we first consider that $V = (v_c n_c + v_b n_b)/(n_c + n_b)$ and:

$$Q = Q_c + Q_b = (v_c n_c + v_b n_b)/L \tag{6}$$

Then, to obtain v_b as function of v_c, we utilize the speed model proposed in [23]:

$$v_b = v_c \frac{s}{s + \tau v_c} \tag{7}$$

where s is the average distance between successive bus stops and τ is the average dwell time at a bus stop. The values of L and τ are network specific. For our tested site L is 200 meters and τ is 25 seconds. Result of the accuracy test of the model (7) shows a good approximation of v_b [23].

Assume first-order approximation in (8), the linearization yields:

$$v_b \cong \theta v_c + \beta \tag{8}$$

where θ and β are parameters. Introducing (8) in (6), we can solve (6) with v_c as the unknown variable and obtain the analytical form of v_c. Thus we obtain the analytical form of Q_c and Q_b as follows:

$$Q_c = \frac{v_c n_c}{L} = \frac{(QL - \beta n_b) n_c}{(n_c + \theta n_b) L} \tag{9}$$

$$Q_b = \frac{v_b n_b}{L} = \left(\frac{QL - \beta n_b}{(n_c + \theta n_b)} \theta + \beta\right) \frac{n_b}{L} \tag{10}$$

Then we derive P by combining (5), (9) and (10):

$$P = h_c n_c \frac{QL - \beta n_b}{(n_c + \theta n_b)} + h_b n_b \left(\frac{QL - \beta n_b}{(n_c + \theta n_b)} \theta + \beta\right) \tag{11}$$

B. The Observation of Passenger Flow Dynamics from Simulated Data

We estimate passenger flow via the simulated data. Denote P' the passenger flows estimated by (5), with the measurements of car flows Q_c, bus flows Q_b and the estimated bus occupancy h_b. We use the same simulated flow data as the ones used to construct Fig. 1(a).

Fig. 4(a) illustrates the 3D-MFD relating accumulation of cars and buses with passenger flow. This figure presents an MFD like-shape for passenger flow. Fig. 4(b) depicts the resulting contour plot of P' on the (n_c, n_b) plane. The polygon in this plot captures the "optimal operational region" of passenger flow of bi-modal traffic. It can be seen that the shape of the region is significantly different from the one observed in Fig. 1(c). More precisely, passenger flow P' first monotonically increases as n_b increases to a critical $\hat{n}_b$ and then decreases for $n_b > \hat{n}_b$. Thus having buses in the network will significantly increase the efficiency of the system but overloading buses will eventually cause delays for all vehicles and reduces passenger throughput. The figure also displays that $\tilde{n}_c$ in this case (rising dotted line in the polygon) has a clear tendency of becoming smaller as n_b increases. The slope of the rising line reflects that only a slight increase of buses can allow a large reduction of cars to maintain the same passenger flow. It can be foreseen that more buses can be deployed in the network to succeed a higher passenger flow if dedicated bus lanes are provided.

We now investigate a functional form of passenger flow 3D-MFD similar to the one obtained for vehicle flow. To this end, we consider the following function:

$$P = a'(n_c + g' n_b) e^{b' n_c^2 + c' n_b^2 + d' n_c n_b + e' n_c + f' n_b} \tag{12}$$

where $a', b', c', d', e', f', g'$ are parameters. The corresponding parameters estimation problem reads (P2):

$$\min_{a,b,c,d,e,f,k} Z = \|\boldsymbol{P} - \boldsymbol{P}'\|^2 \tag{13}$$

Subject to $P \geq 0$

Solving P2, we get $a', b', c', d', e', f', g'$ = 6.41e-10, -2.27e-06, -1.14e-07, -3.77e-04, -5.30e-04, 3.658, 3.46e02. Fig**.** 5(a) depicts the result of the fitting model (12) with the parameters. An R-test value of 0.91 (close to 1) indicates well model fitting. Fig. 5(b) depicts the contour plot of the 3D surface on the (n_c, n_b) plane. Fig**.** 5(b) shows consistency with the three observations made in Fig. 4(b).

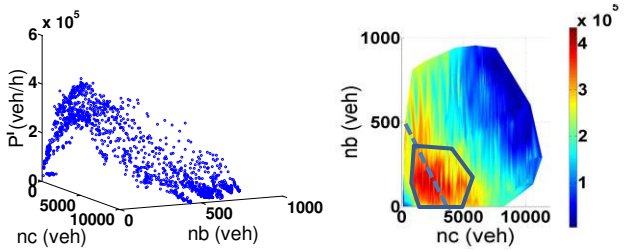

Fig. 4. (a) The 3D-MFD for bi-modal passenger traffic; (b) Contour plot of the 3D-MFD

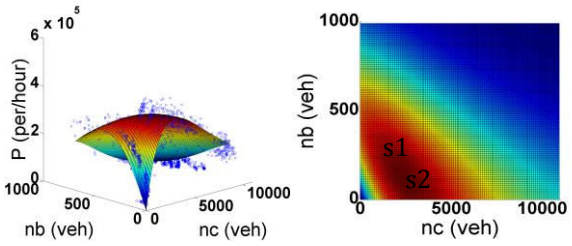

Fig. 5. (a) The approximated passenger flow 3D-MFD; (b) Contour plot of the 3D-MFD on the $(\boldsymbol{n_c}, \boldsymbol{n_b})$ plane.

IV. The Macroscopic Fundamental Diagram for Buses Operating in Dedicated Lanes

The efficiency of transporting people in multimodal networks may be further improved if dedicated bus lanes are provided. In this case, the interactions between cars and buses are much smaller and buses can travel faster in these lanes. Nevertheless, if this is not associated with high occupancy of buses and high frequency, this space will be underutilized. We now investigate if a city-wide relation between flow and density of buses (MFD for buses) exist for urban networks where buses running in dedicated lanes. To this end, the test site is updated and one lane in each road of the city center is dedicated to buses. The resulted bus-lane network is well connected and includes about 5 km of dedicated bus lanes. To derive and investigate the shape of the MFD for buses, simulations are performed with a field-applied fixed-time plan and fixed number of bus lines. To account for demand effects of the bi-modal traffic composition, ten runs were carried out for a 4-h time-dependent scenario with different car demand and bus frequency. Additionally, two scenarios based on different dwell time of buses were defined in order to investigate the impact of the dwell time in the shape of the MFD for buses.

Fig. 6 displays the MFD for buses resulting for the aforementioned runs. This figure plots the flow-density relationship (buses/5min vs. buses/km) in the network for the whole simulation time period. Each measurement point in the diagram corresponds to 5 minutes. Fig. 8 confirms the existence of an MFD for buses with moderate scatter across different runs. However, the flows show a significant scattering in the congested regime. It can be seen that the free flow speed in the bus lanes is around 40 km/h and the

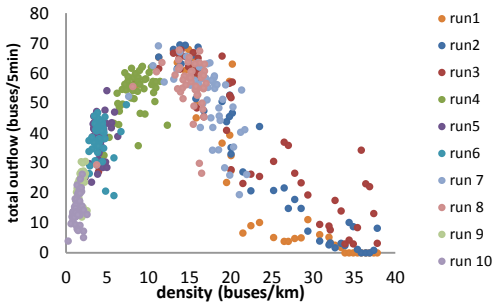

Fig. 6. The MFD for buses for ten runs with different bi-modal traffic patterns.

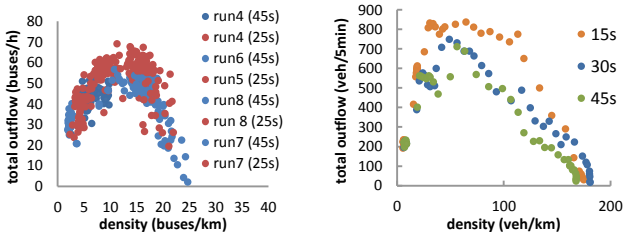

Fig. 7. The impact of different average dwell time of buses in the MFD: (a) MFD for buses; (b) MFD for the mixed traffic.

maximum flow occur in a density range from 10 to 20 buses per km. A critical density $\hat{n}_b$ can be observed at 15 buses per km. If the density is allowed to increase to values $n_b > 15$, then the dedicated bus lanes become severely congested, the flow decreases with density (negative slope) and the network can lead to gridlock. This MFD like-shape for buses operating in dedicated lanes is quite conforming to the MFD for cars and mixed traffic. An interesting observation is that the diagram indicates a high flow scatter for the critical bus density $\hat{n}_b$. This difference is attributed to different traffic patterns for the cars and the interaction of the bi-modal traffic at the intersections that could lead to partially block of the dedicated bus lanes due to spillbacks.

Besides bus frequency, the effect of the dwell times in the shape of the MFD is analyzed as longer dwell times reduce the average speed and flow. Fig. 7 illustrates the impact of different dwell time of buses in the MFD. Fig. 7(a) plots the MFD for buses resulting for 8 runs, where half runs have average dwell time of 25 s and the other 45 s, while Fig. 7(b) plots the MFD for 3 runs for the whole network (mixed traffic). It can be seen in both diagrams that the use of smaller dwell time leads to higher flow capacity, as expected. In order to derive more reliable conclusions regarding the impact of different factors to the shape of the MFD for buses and the whole network, more experiments will be carried at a more advanced stage of this research.

V. Discussion

In this paper, we extended the single-mode Macroscopic Fundamental Diagram model to a bi-modal (bus and cars) one, with the consideration of passenger flows in addition to vehicle flows. We investigated the relation between the

accumulation of cars and buses, and the vehicle flow throughput of the network via a 3D-MFD. This 3D-MFD was developed and parameterized for both vehicle throughput and passenger throughput. We have shown via simulation experiments that: (i) an exponential family function fits well the data points, (ii) the network's vehicle throughput decrease monotonically by increasing the number of buses serving in the network; (iii) the passenger throughput is maximized at a non-zero accumulation of buses. Furthermore, we investigated the dedicated bus-lane MFD and the impact of bus operational characteristics in the shape of the MFD.

The findings of this paper are promising because the concept of a 3D-MFD can be used: (i) to monitor traffic performance in bi-modal networks, and traffic flow dynamics can be predicted given the current state of the two modes, (ii) towards the development of simple control policies in such a way that maximizes the bi-modal network vehicle flow or passenger throughput and (iii) towards the expression of PCU as a functions of the bi-modal traffic in the network. Moreover, the proposed bus MFD can be used for estimating buses delays and designing dedicated bus lanes. In particular, policy makers can adjust management measures to operate at different mobility levels as expressed by the MFD in Fig. 6(b). Example cases are referred as "s1" and "s2" in Fig. 5(b) with similar passenger flows. Policy-makers can choose to operate at state "s1", where a higher number of buses are in service compared to scenario "s2" in the network. One of the advantages is the reduction in emissions and fuel consumption as a result of fewer cars on the road. An expansion in the bus fleet of a city associated with a congestion pricing scheme to facilitate demand shift from cars to buses can succeed these goals. Further research is needed towards this direction. Ongoing work investigates how perimeter control of cars can improve the system operation and decrease total passenger delays. Bus priority strategies are also investigated.

ACKNOWLEDGEMENT

This research was financially supported by the Swiss National Science Foundation (SNSF) grant # 200021-132501.

REFERENCES

[1] C. Daganzo and M. Cassidy, "Effects of high occupancy vehicle lanes on freeway congestion," *Transport Research Part B*, Vol. 42, No. 10, pp. 861-872, 2008.

[2] J. Li, M. Song and W. Zhang, "Planning for bus rapid transit in single dedicated bus lane," *Transportation Research Record*, Vol. 2111, pp. 76-82, 2010.

[3] M. Mesbah and G. Currie, "Optimization of transit priority in the transportation network using a genetic algorithm," *IEEE Trans.on Intelligent Transportation Systems*, Vol. 12, No. 3, pp. 908-919, 2011.

[4] M. Eichler and C. Daganzo, "Bus lanes with intermittent priority: Strategy formulae and an evaluation," *Transport Research Part B*, Vol. 40, No. 9, pp. 731-744, 2006.

[5] K. Tuerprasert and C. Aswakul, "Multiclass cell transmission model for heterogeneous mobility in general topology of road network," *Journal of Intelligent Transport Systems: Technology, Planning, and Operations*, Vol. 14, No. 2, pp. 68-82, 2010.

[6] J. Godfrey, "The mechanism of a road network," *Traffic Engineering and Control*, Vol. 11, No. 7, pp.323-327, 1969.

[7] H. Mahmassani, J. Williams and R. Herman, "Performance of urban traffic networks," in *Proc. 10th Int. Symp. on Transportation and Traffic Theory*, Amsterdam, The Netherlands, 1987, pp. 1-20.

[8] C. Daganzo, "Urban gridlock: macroscopic modeling and mitigation approaches," *Transportation Research Part B,* Vol. 41, No. 1, pp. 49-62, 2007.

[9] N. Geroliminis and C. Daganzo, "Existence of urban-scale macroscopic fundamental diagrams: some experimental findings," *Transportation Research Part B*, Vol. 42, No. 9, pp. 759-770, 2008.

[10] A. Mazloumian, N. Geroliminis and D. Helbing, "The spatial variability of vehicle densities as determinant of urban network capacity," *Philosophical Transactions of Royal Society A*, Vol. 368, No. 1928, pp. 4627-4648, 2010.

[11] C. Daganzo, V. Gayah and E. Gonzales, "Macroscopic relations of urban traffic variables: bifurcations, multivaluedness and instability," *Transportation Research Part B,* Vol. 45, No. 1, pp. 278-288, 2011.

[12] C. Daganzo and N. Geroliminis, "An analytical approximation for the macroscopic fundamental diagram of urban traffic," *Transportation Research Part B*, Vol.42, No. 9, pp. 771-781, 2008.

[13] N. Geroliminis and B. Boyaci, "The effect of variability of urban systems characteristics in the network capacity," *Transportation Research Part B,* Vol. 46, No. 10, pp.1607–1623, 2012.

[14] C. Buisson and C. Ladier, "Exploring the impact of homogeneity of traffic measurements on the existence of Macroscopic Fundamental Diagrams," *Transportation Research Record*, Vol. 2124, pp. 127-136, 2009.

[15] Y. Ji, W. Daamen, S. Hoogendoorn, S. Hoogendoorn-Lanser, and X. Qian, "Macroscopic fundamental diagram: investigating its shape using simulation data," *Transportation Research Record*, Vol. 2161, pp. 42-48, 2010.

[16] N. Geroliminis and J. Sun, "Properties of a well-defined macroscopic fundamental diagram for urban traffic," *Transportation Research Part B,* Vol. 45, No. 3, pp. 605-617, 2011.

[17] M.Saberi and H. Mahmassani, "Exploring properties of network-wide flow-density relations in a freeway network," *Transportation Research Record*, No. 2315, pp. 153-163, 2012.

[18] Y. Ji and N. Geroliminis, "On the spatial partitioning of urban transportation network," *Transportation Research Part B*, Vol. 46, No. 10, pp. 1639-1656, 2012.

[19] V. Knoop, S. Hoogendoorn and H. van Lint, "The impact of traffic dynamic on the Macroscopic Fundamental Diagram," in *Proc. 92nd Annual Meeting of Transportation Research Board*, Washington D.C., USA, 2013.

[20] M. Keyvan-Ekbatani, A. Kouvelas, I. Papamichail and M. Papageorgiou, "Exploiting the fundamental diagram of urban network for feedback-based gating," *Transport Research Part B*, Vol. 46, No.10, pp. 1393-1403, 2012.

[21] N. Geroliminis, J. Haddad and M. Ramezani, "Optimal Perimeter Control for Two Urban Regions with Macroscopic Fundamental Diagrams: A Model Predictive Approach," *IEEE Transactions on Intelligent Transportation Systems*, Vol. 14, No.1, pp. 348-359, 2012.

[22] N. Zheng, R. Waraich, K. Axhausen and N. Geroliminis, "A dynamic cordon pricing scheme combining the Macroscopic Fundamental Diagram and an agent-based traffic model," *Transportation Research Part A*, Vol. 46, No. 8, pp. 1291–1303, 2012.

[23] N. Zheng and N. Geroliminis, "On the distribution of urban road space for multimodal congested networks," in *Proc. 20th Int. Symp. on Transportation and Traffic Theory*, Noordwijk, the Netherlands, 2013.

[24] E. Gonzales, C. Chavis, Y. Li and C. Daganzo, "Multimodal Transport in Nairobi, Kenya: Insights and Recommendations with a Macroscopic Evidence-Based Model," in *Proc. 90th Annual Meeting Transportation Research Board*, Washington, D.C., USA, 2011.

[25] E. Gonzales and C. Daganzo, "Morning commute with competing modes and distributed demand: User equilibrium, system optimum, and pricing," *Transportation Research Part B*, Vol. 46, No. 10, pp. 1519-1534, 2012.

[26] K. Aboudolas and N. Geroliminis, "Feedback perimeter control for multiregion and heterogeneous congested cities," in *Proc. 92nd Annual Meeting of Transportation Research Board*, Washington D.C., USA, 2013.